3 Correlation Spectroscopy of Nano-size Materials

Oleg Kidun, Natasha Fominykh, and Jamal Berakdar

3.1 Introduction

The role of the Coulomb interaction in determining the physical properties of electronic materials has been the subject of research since the early days of modern physics. The everlasting interest in this topic is not only due to the complexity and the intellectual challenge in describing interacting, many electron systems. A variety of observable physical phenomena are shown to be dominated by electronic correlation: Wannier excitonic states in wide-bandwidth semiconductors are caused by the Coulomb interactions, whereas in narrow band materials, such as in 3d transition metal oxides, rare earths, or actinides, the Coulomb interactions may lead to insulating (magnetic) ground states. The understanding of the influence of the electronic interaction in molecular and polymeric materials has also been a major topic of research. E.g., the discovery that C_{60} doped with alkali metals may acquire a superconducting state [1] sparked a large body of investigations of the role of the electron–electron (e–e) interaction in this molecular material: Analyzing the KVV C_{60} Auger results it has been concluded [2] that doped C_{60} has the properties of a strongly correlated system, e.g. it has been argued that K_3C_{60} is a half-filled Mott–Hubbard insulator. A theoretical study of the nature of the e–e interaction in solid (ordered) phase C_{60} concluded that the screened on-site molecular Coulomb integral U is ≈ 2.1 eV [3]. A step forward in uncovering the features of the e–e interaction in C_{60} has also been made in Ref. [4] where the screening of the e–e interaction has been studied within the random phase approximation (RPA) using a simplified model of C_{60}. As is well-known and discussed below, screening effects can be quantified by the dielectric function. From experimental results for C_{60} estimated values for the macroscopic dielectric function (defined below) have been given as 4.6 in Ref. [5] and 3.6 in Ref. [6], indicating that in *solid* C_{60} screening is weak. However, these numbers do not reflect on the real facets of the e–e interaction screening, in particular as far as on-site screening and screening of the e–e interaction in isolated fullerenes are concerned. These issues will be discussed in some detail in the present chapter. In this context it is worthwhile to recall the general significance of the concept of screening: the theoretical challenges in such diverse and important phenomena as high-T_c in cuprates, the colossal magnetoresistance, Kondo impurity and Kondo lattice problems stem from the fact that the Coulomb interactions involving the valence electrons are not sufficiently screened which makes imperative the use of truly many-body techniques. Thus, ways and methods to investigate theoretically and experimentally details of the electron–electron interaction and its screening are highly desirable. Of special interest in this chapter are the effects of dimensionality and the finite size of the system. In addition it should be emphasized here that the approach we will follow in studying the properties of the electron–electron interaction relies on non-number conserving excitations (electron-removal spectroscopy). In contrast most of the theoretical and experimental studies of the dielectric properties of electronic systems are based on neutral excitations, as done in electron energy-loss spectroscopy (EELS) or photoabsorption spectroscopy. Such studies are the subject of the Chapter 2 by Marini. Here we will only mention some aspects of direct relevance to the material presented in this chapter.

Correlation Spectroscopy of Surfaces, Thin Films, and Nanostructures. Edited by Jamal Berakdar, Jürgen Kirschner

ISBN: 3-527-40477-5

3.2 Generalities

The most used approach to the treatment of screening effects in solids is to replace the discrete atomic lattice by a uniform medium. The second step is then to employ a self-consistent mean-field treatment of a wave-vector dependent dielectric function $\epsilon(q)$. For ionic insulators one usually utilizes the Clausius–Mossotti derivation of a dielectric constant in terms of the atomic polarizabilities, which leads to a linear suppression of the e–e interaction u by the dielectric function ($U_{\rm eff} = u/\epsilon(q)$). In this approach the screened potential $U_{\rm eff}$ is a function only of the relative distance between the charges, effects due to the crystal structure as well as local-field corrections are neglected. Furthermore, wave vector-dependence of ϵ is often disregarded, i.e. all effects of screening are subsumed in a reduction of the Coulomb interaction by a constant amount. The deficiencies of the methodology of a uniform dielectric theory become apparent when one attempts to estimate the amount of screening between electrons on the same site (atoms) or when one is interested in local field effects. At first glance it may appear that screening between electrons on one site can be neglected due to the absence of a surrounding polarizable medium and because the confinement of the systems leads to electronic energy-level quantization with considerable level spacing, i.e. excitation and de–excitation of electron–hole pairs may be less effective. However, as shown below for some molecules and clusters, e.g. C_{60} the amount of screening may be as large as in conventional metals.

Before presenting our approach to study the e–e interaction screening in large molecules and clusters it is instructive to recall some of the calculational aspects widely used to treat screening in semiconductors. Mostly the calculations are based on density functional theory (and the local-density approximation). The electronic contributions to the static dielectric function are evaluated as [7]

$$\epsilon^{-1}(\boldsymbol{r},\boldsymbol{r}') = \delta(\boldsymbol{r},\boldsymbol{r}') + \int \mathrm{d}\boldsymbol{r}''\, u(\boldsymbol{r},\boldsymbol{r}'')\chi(\boldsymbol{r}'',\boldsymbol{r}')\,. \tag{3.1}$$

The polarizability χ is determined as [1]

$$\chi = (1 - \chi_0 u - \chi_0 K_{\rm xc})^{-1}\chi_0\,. \tag{3.2}$$

[1] These expressions for the inverse dielectric function are appropriate when the "test charge" is external to the electronic system that is polarized by this test charge (as the case considered here). If the system response is to be probed by the electrons contained in the system one has to evaluate ϵ as $\epsilon^{-1} = 1 + (u + K_{\rm xc})\chi$.

For a semiconductor the independent particle polarizability χ_0 is expressed as the Fourier transform

$$\chi_{GG'}(q) = 4\sum_{\mathrm{v,c}} \frac{\langle\psi_\mathrm{v}|\mathrm{e}^{-i(q+G)\cdot r}|\psi_\mathrm{c}\rangle\langle\psi_\mathrm{c}|\mathrm{e}^{-i(q+G')\cdot r}|\psi_\mathrm{v}\rangle}{\epsilon_\mathrm{v} - \epsilon_\mathrm{c}}. \tag{3.3}$$

ψ_v and ψ_c are the valence and conduction band wavefunctions with associated energies ϵ_v and ϵ_c. Exchange and correlation effects in the system response are incorporated in Eq. (3.2) via the exchange and correlation functional K_xc (more precisely the term K_xc can be determined from $K_\mathrm{xc}(\boldsymbol{r},\boldsymbol{r}') = \frac{\mathrm{d}V_\mathrm{xc}}{\mathrm{d}\rho}\Big|_{\rho(\boldsymbol{r})} \delta(\boldsymbol{r}-\boldsymbol{r}')$, where ρ is the electronic density and V_xc is the exchange-correlation potential). The assumption in Eq. (3.2) that $K_\mathrm{xc} = 0$ amounts to the random phase approximation (RPA), i.e. within the RPA no account is taken of the exchange and correlation on the polarizability of the inhomogeneous electron gas[2] (we note however, that such effects are partially incorporated in the ground state calculations of ψ_v and ψ_c). The polarizability (Eq. (3.2)) is then directly dependent on the independent particle polarizability χ_0. The latter is determined by excitation and de-excitations between the valence and the conduction band (3.3) due to a Born-type perturbation. In most cases this term is evaluated for neutral excitations. Below we propose a way to calculated χ_0 for a finite system (C_{60} and metal clusters) while taking into account the effects of exchange on the polarizability (and on the ground state wavefunctions).

3.3 Excitations in Finite Systems: Role of the Electron–Electron Interaction

In a series of experiments [13,14] the probability for the removal of one electron from the valence band of the carbon fullerenes (C_{60}) has been measured by bombarding it with electrons. Density functional calculations (DFT) with the local density approximation (without RPA) as well as Hartree–Fock calculations failed to reproduce the excitation probability as a function of the excitation energy [15–17]. Thus an obvious step to remedy (or at least to improve) this situation is to evaluate the removal probability within RPA. However, DFT calculations with RPA for removal probabilities turned out to be computationally very demanding and have not yet been performed. We followed another route by adopting a self-consistent Hartree–Fock procedure, using the so-called variable-phase method to deal with a large number of electrons, and performed an RPA procedure appropriate to electron removal processes. The RPA we use is similar in spirit to the conventional one presented in the preceding section, however we were able to incorporate the effect of exchange on the polarizability which has important consequences on the calculated response of the system, depending on the nature of the probing charge.

[2] The macroscopic response of the system ϵ_M is given by the diagonal elements of the inverse dielectric function [8] $\epsilon^{-1}_{GG}(q)$, i.e. by $(1/\left[\epsilon^{-1}_{GG}(q)\right])$. Hence it depends on the non-diagonal elements of ϵ, usually referred to as local fields [9]. The macroscopic dielectric function is determined from the long-wave length limit of ϵ_M (i.e. for $q \to 0$).

3.3.1 Formal Development

Consider a cluster of atoms under the influence of an external time-dependent perturbation $U(\boldsymbol{r},t)$ that couples to the electronic part of the cluster Hamiltonian. The perturbation may be induced by an impinging electron (that acts as a test charge) or by an electromagnetic pulse. We are interested in the characteristic response of the system quantified in terms of electron removal probabilities from the valence shell.

The dynamic of the electrons in the cluster is governed by the Hamiltonian

$$\widehat{H}(\boldsymbol{r},t) = \widehat{H}_0(\boldsymbol{r}) + U(\boldsymbol{r},t), \tag{3.4}$$

where $\widehat{H}_0$ is the self-consistent mean field Hamiltonian in the absence of the perturbation. The solution $\Psi(\boldsymbol{r},t)$ of the time-dependent Schrödinger equation (atomic units are used throughout)

$$\left[i\partial_t + \widehat{H}(\boldsymbol{r},t)\right]\Psi(\boldsymbol{r},t) = 0 \tag{3.5}$$

is written as an antisymmetrized product of single-electron wavefunctions, i.e.

$$\Psi(\boldsymbol{r},t) = \mathrm{e}^{-iE_0 t}\det\|\psi_i(\boldsymbol{r},t)\|\,. \tag{3.6}$$

Here E_0 is the Hartree–Fock energy of the ground state. The value of E_0 is determined as the expectation value (recall that $u \equiv \frac{1}{|\boldsymbol{r}-\boldsymbol{r}'|}$ and the ionic potential experienced by the electrons is denoted by V_ions)

$$E_0 = \sum_i \langle i|-\frac{\nabla}{2} - V_\mathrm{ions}|i\rangle + \frac{1}{2}\sum_{i,k}\langle ik|\,u\,|ik-ki\rangle\,. \tag{3.7}$$

The time dependent single particle orbitals $\psi_i(\boldsymbol{r},t)$ are then expanded in term of time-independent Hartree–Fock orbitals

$$\psi_i(\boldsymbol{r},t) = A_i\left[\phi_i(\boldsymbol{r}) + \sum_m C_{mi}(t)\phi_m(\boldsymbol{r})\right]. \tag{3.8}$$

The index m refers to states above Fermi level E_F (particle states) whereas i labels the states below E_F (hole states). The factor A is a normalization coefficient. From the meaning of the indices i and m one concludes that the expansion coefficients $C_{mi}(t)$ are the probability amplitudes for the creation of the m–i electron–hole pair. The sum in Eq. (3.8) implies a summation over discrete states and an integration over the continuum (particle) states. To obtain a determining equation for the particle–hole excitation amplitudes $C_{mi}(t)$ one inserts Eq. (3.8) into Eq. (3.6) and requires that

$$\langle\Psi(\boldsymbol{r},t)|\,\widehat{H} - i\frac{\partial}{\partial t}\,|\Psi(\boldsymbol{r},t)\rangle \equiv 0. \tag{3.9}$$

Expanding in $C_{mi}(t) \neq 0$ and accounting for the first non-vanishing terms one obtains the relation

$$
\begin{aligned}
i \sum_{i\le\varepsilon_F<m} C^*_{mi}(t)\frac{\partial}{\partial t}C_{mi}(t) = \sum_{i\le\varepsilon_F<m}\Bigg\{ & (\varepsilon_m-\varepsilon_i)\,|C_{mi}(t)|^2 \\
& + C_{mi}(t)\,\langle i|\,U\,|m\rangle + C^*_{mi}(t)\,\langle m|\,U\,|i\rangle \\
& + \sum_{j\le\varepsilon_F<k}\Bigg[\frac{1}{2}C^*_{mi}(t)C^*_{kj}(t)\,\langle mk|\,u\,|ij-ji\rangle \\
& + \frac{1}{2}C_{mi}(t)C_{kj}(t)\,\langle ij|\,u\,|mk-km\rangle \\
& + C^*_{mi}(t)C_{kj}(t)\,\langle mi|\,u\,|kj-kj\rangle\Bigg]\Bigg\}.
\end{aligned}
\tag{3.10}
$$

The variation with respect to $C^*_{mi}(t)$ results in the relation

$$
\begin{aligned}
i\frac{\partial}{\partial t}\,C_{mi}(t) = (\varepsilon_m-\varepsilon_i)\,C_{mi}(t) + \langle m|\,U\,|i\rangle + \\
\sum_{j\le\varepsilon_F<k}\left[C^*_{kj}(t)\,\langle mk|\,u\,|ij-ij\rangle + C_{kj}(t)\,\langle mj|\,u\,|ik-ki\rangle\right].
\end{aligned}
\tag{3.11}
$$

Solutions of this equation are expressed as

$$
C_{mi}(t) = X_{mi}e^{-i\varepsilon_0 t} + Y^*_{mi}e^{i\varepsilon_0 t},
\tag{3.12}
$$

where ε_0 is the energy imparted by the external perturbation (the incoming projectile). With the ansatz (3.12) we obtain from Eq. (3.11) two coupled equations for the determination of the coefficients X_{mi} and Y^*_{mi}, namely

$$
\begin{aligned}
(\varepsilon_m-\varepsilon_i-\varepsilon_0)\,X_{mi} + \langle m|\,U\,|i\rangle \\
+\sum_{j\le\varepsilon_F<k}\left[\langle mj|\,u\,|ki-ik\rangle\,X_{kj} + \langle mk|\,u\,|ji-ij\rangle\,Y_{kj}\right] = 0,
\end{aligned}
\tag{3.13}
$$

$$
\begin{aligned}
(\varepsilon_m-\varepsilon_i+\varepsilon_0)\,Y_{mi} + \langle i|\,U\,|m\rangle \\
+\sum_{j\le\varepsilon_F<k}\left[\langle ij|\,u\,|km-mk\rangle\,X_{kj} + \langle ik|\,u\,|jm-mj\rangle\,Y_{kj}\right] = 0.
\end{aligned}
\tag{3.14}
$$

Now we introduce the following definitions for the effective transition amplitudes

$$
-(\varepsilon_m-\varepsilon_i-\varepsilon_0)X_{mi} =: \langle m|\,U_{\rm eff}\,|i\rangle\,, \tag{3.15}
$$

$$
-(\varepsilon_m-\varepsilon_i+\varepsilon_0)Y_{mi} =: \langle i|\,U_{\rm eff}\,|m\rangle\,. \tag{3.16}
$$

This means that $U_{\rm eff}$ acts as an *effective* external perturbation. Its structure is determined by the naked perturbation and by the particle–hole excitation and de-excitation amplitude. The

exact expression for $U_{\rm eff}$ derives from Eqs. (3.13), (3.14), namely

$$
\begin{aligned}
\langle m|\,U_{\rm eff}\,|i\rangle = \langle m|\,U\,|i\rangle + \\
\sum_{j\le\varepsilon_F<k}\left[\frac{\langle k|\,U_{\rm eff}\,|j\rangle\,\langle mj|\,u\,|ki-ik\rangle}{\varepsilon_0-\varepsilon_k+\varepsilon_j+i\nu} + \frac{\langle j|\,U_{\rm eff}\,|k\rangle\,\langle mk|\,u\,|ji-ij\rangle}{\varepsilon_0+\varepsilon_k-\varepsilon_j-i\nu}\right].
\end{aligned}
\tag{3.17}
$$

Taking into account that in a linear-response theory $U_{\rm eff} = \epsilon^{-1}U$ and comparing with Eqs. (3.1)–(3.3) one sees that the approach derived here is equivalent to the RPA, however in the present approach exchange effects on the polarizability are accounted for. We recall that within the HF approximation exchange effects are taken exactly into account but correlation is not accounted for. In contrast, within DFT-LDA exchange and correlation effects are described in an approximate way through the employed exchange and correlation functional. This advantage of the HF comes of the expense of evaluating the expectation value of a large number of non-local potentials (Fock terms) [17, 18]. It turns out that the numerical problems arising from the non-locality of the potentials can be circumvented by utilizing the variable-phase method (VPM). For this purpose we developed a version of VPM applicable to non-local potentials, details are presented in Ref. [19].

3.4 Results and Discussion

A way to test in details (theoretically and experimentally) the features of the matrix elements of the effective interaction $U_{\rm eff}$ is to approach the sample (residing in the initial state ϕ_ν) with a test charge (described by the state vector $|\boldsymbol{k}_0\rangle$, where $\boldsymbol{k}_0$ is the wave vector of the incoming projectile). The impinging test charge acts on the sample with the perturbation U (usually known in its naked form). This causes the removal of one electron from the bound state (ϕ_ν) into a continuum state, characterized by $|\boldsymbol{k}_1\rangle$, where $\boldsymbol{k}_1$ is the wave vector of the emitted electron. The final-state wave vector of the projectile is denoted by $\boldsymbol{k}_2$. According to Eq. (3.17) we write the transition amplitude for this reaction as $T = \langle \boldsymbol{k}_1\boldsymbol{k}_2|U_{\rm eff}|\phi_\nu\boldsymbol{k}_0\rangle$. If electrons are used as a projectile the observable quantity is a spin averaged, differential cross section $W(\boldsymbol{k}_0;\boldsymbol{k}_1,\boldsymbol{k}_2)$ evaluated as the weighted average of the singlet $\propto |T^{(S=0)}|^2$ (vanishing total spin ($S=0$) of the electron pair) and the triplet $\propto |T^{(S=1)}|^2$ cross sections. Assuming spin-flip processes to be irrelevant, the total cross section $W(\epsilon_0)$ is accordingly given as

$$
\begin{aligned}
W(\epsilon_0) = \frac{(2\pi)^4}{k_0}\int \mathrm{d}^3\boldsymbol{k}_1\mathrm{d}^3\boldsymbol{k}_2\Bigg\{\sum_\nu\frac{1}{4}\left|T^{(S=0)}(\boldsymbol{k}_0,\phi_\nu;\boldsymbol{k}_1,\boldsymbol{k}_2)\right|^2 + \\
\frac{3}{4}\left|T^{(S=1)}(\boldsymbol{k}_0,\phi_\nu;\boldsymbol{k}_1,\boldsymbol{k}_2)\right|^2\delta\left(\epsilon_0+\epsilon_\nu-(k_1^2/2+k_2^2/2)\right)\Bigg\}.
\end{aligned}
\tag{3.18}
$$

If projectiles other than electrons are employed, the exchange part of the cross section vanishes.

Below we present results for the scattering cross section from C_{60} and metal clusters. Using the spherical jellium model [10, 11] we construct the quantum states of the clusters in

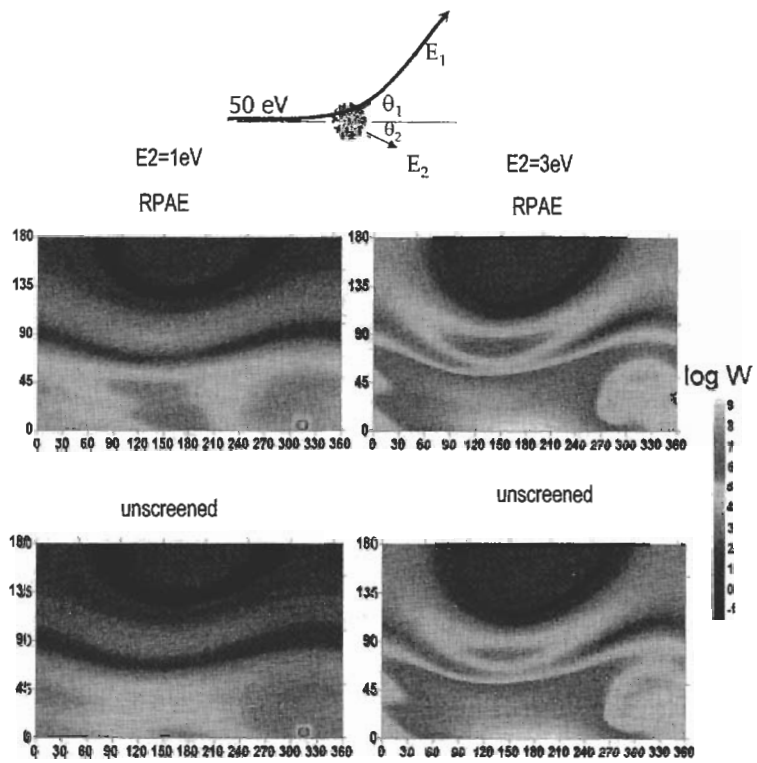

Figure 3.1: The angular dependence of the fully differential cross section for the emission of one electron from C_{60} with 1 eV (left panel) or 3 eV (right panel) following the impact of 50 eV electrons. A schematic of the scattering geometry is depicted. The upper part of the figure shows the RPAE calculation while the lower part shows the calculations without treating screening effects. See also color figure on page 226.

the framework of the Hartree–Fock approximation. The cluster potential (the superposition of atomic potentials) is replaced by a shell confinement. The delocalized valence electrons of carbon atoms are subject to the potential well: $V(r) = V_0$ within the region $R - \Delta < r < R + \Delta$, and $V = 0$ elsewhere. For C_{60} we use $R \approx 6.7\ a_0$ as the radius of the fullerene. The thickness of the shell is $2\Delta \approx 2\ a_0$ (a_0 is the Bohr radius). The height of the well is determined such that the experimental value of the electron affinity of C_{60}^+ and the number of valence electrons are correctly reproduced. A model cluster potential as derived from density functional theory (DFT) within the local density approximation [16] is

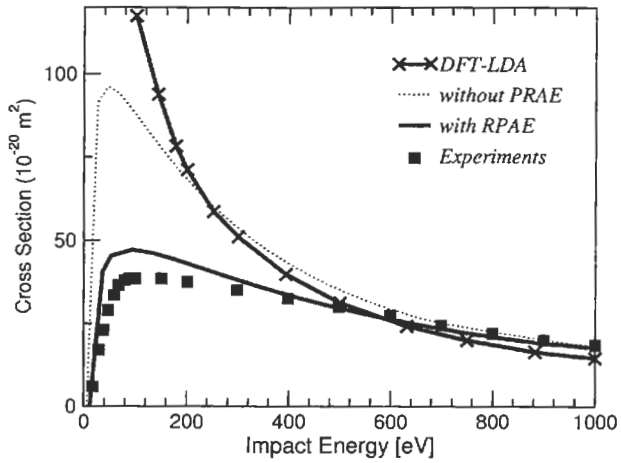

Figure 3.2: The absolute total cross section for the removal of one electron from C_{60} upon the inelastic collision of electrons with the impact energy displayed on the axis. The experimental data (full squares) are taken from Refs. [13,14]. The solid curve with crosses is the result of DFT calculations [15] whereas the dotted curve shows the present theory without RPAE. Theoretical results based on RPAE are shown by the solid curve.

shown to lead to essentially the same conclusions [17]. As demonstrated in Refs. [15, 16], the large extent of C_{60} and the large number of electrons to be considered (240 e^-) results in severe convergence problems in evaluating the transition matrix elements. A way around this problem is to use the non-local variable phase approach [12, 19] for the numerical calculation of the Hartree–Fock states. Upon numerical summation over the states ϕ_ν in Eq. (3.18) one obtains the differential cross sections. To evaluate the total cross section we carry out the six-dimensional integral over the momenta $\boldsymbol{k}_1$ and $\boldsymbol{k}_2$ (cf. Eq. (3.18)) using a Monte-Carlo procedure. Figure 3.1 shows the angular dependence of the fully differential cross section $W(\boldsymbol{k}_0; \boldsymbol{k}_1, \boldsymbol{k}_2)$ for C_{60}. The calculations are performed with (upper part in Figure 3.1 and without (lower part in Figure 3.1 inclusion of RPAE (RPA with exchange). In general, the rough structure of the cross section is similar in both cases. The effect of screening is to reduce and broaden some of the peaks. With increasing scattering angle θ_1 of the projectile electron the amount of transferred momentum q to the target increases. Since the response of the system is strongly dependent on the amount of transferred momentum, we observe that the RPA correction are significant only for a certain range of the transferred momentum.

The same applies to the transferred energy dependence of the cross section. This behavior is still observable in the total cross section (Figure 3.2). In the high energy regime there is hardly a difference between the calculations with and without RPA. This is because the time scale for the retarded response of the sample is far off the very short passage time of keV electrons. However at lower energies we observe a strong dependence on screening, in

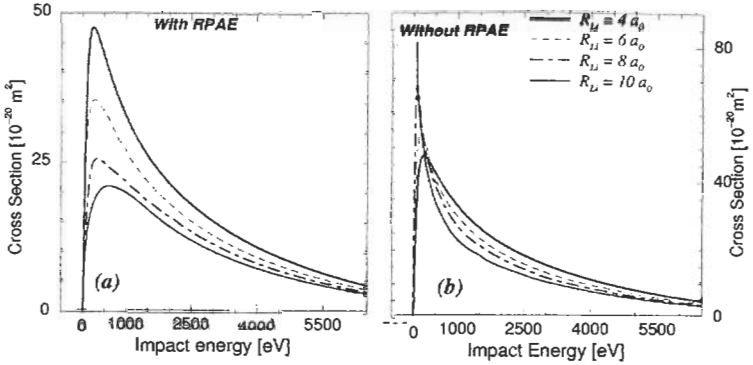

Figure 3.3: The electron-impact ionization cross section for spherical Li clusters with varying radius size R_{Li}. (a) shows the RPAE calculations. (b) shows the results when the particle–hole (de)excitation is neglected.

particular the shape of the cross section is modified. Hence screening of the electron–electron interaction cannot be modelled by a constant suppression of the Coulomb interaction (U/ϵ) since this will lead to a mere energy-independent lowering of the cross section. Figures 3.1 and 3.2 illustrate the ability of the two-electron coincidence technique in mapping the details of the screened electron–electron interaction in small systems, in particular the angular dependence shown in Figure 3.1 is unique to this technique and can not be accessed by other methods such as EELS or photoabsorption spectroscopy.

One of the aims in developing the above theory is to address the system size dependence on the screening of the electron–electron interaction. This is done by considering within the spherical jellium model the electron-removal amplitudes from Li clusters with varying sizes. The cross sections depicted in Figure 3.3 are normalized to the number of electrons in the respective clusters. As evident from Figure 3.3, for small clusters there is hardly any influence of the particle–hole (de)excitations and hence the calculations with and without RPAE are almost identical. On the other hand, with increasing system size the influence of charge density fluctuation (described by the the particle–hole (de)excitations) has a strong influence on the cross section, in particular at low energies.

Contrary to the intuitive expectation, the normalized cross section decreases with increasing cluster size. This is due to an enhanced screening strength, meaning that the effective interaction U_{eff} is reduced. Thus, the scattering region shrinks and consequently the associated cross section decreases.

3.5 Conclusions

This chapter presented a brief overview of how the screening of the electron–electron interaction in finite, nano-size materials can be treated theoretically. The method of choice to map out the details of the electron–electron interaction is the coincident detection of the quantum states of an impinging test charge and a knocked-out electron from the sample. Numerical examples have been presented that illustrate the energy and the angular dependence of the screening effects as well as the dependence on the system size. It should be noted that the calculational examples are the results of the first-order term in a perturbation expansion (cf. Section 3.3.1). In principle the reliability of the results should be assessed by evaluating the contributions of higher-order terms. However the numerical calculations of these terms are far more computationally demanding than RPA and have not yet been explored.

References

[1] A. F. Hebard, M. J. Rosseinsky, R. C. Haddon, D. W. Murphy, S. H. Glarum, T. T. M. Palstra, A. P. Ramirez, A. R. Kortan, Nature **350** (1991) 600.

[2] R. W. Lof, M. A. van Veenendaal, B. Koopmans, H. T. Jonkman, G. A. Sawatzky, Phys. Rev. Lett. **68** (1992) 3924; R. W. Lof, M. A. van Veenendaal, H. T. Jonkman, G. A. Sawatzky, J. Electron Spectrosc. Relat. Phenom. **72** (1995) 83.

[3] D. P. Joubert, J. Phys.: Condens. Mater **5** (1993) 8047.

[4] O. Gunnarsson and G. Zwicknagel, Phys. Rev. Lett. **69** (1992) 957.

[5] P. L. Hansen, P. J. Fallon, W. Kratschmer, Chem. Phys. Lett. **181** (1991) 367.

[6] S. L. Ren, Y. Wang, A. M. Rao, E. McRae, J. M. Holden, T. Hager, KaiAn Wang, Wen-Tse Lee, H. F. Ni, J. Selegue, P. C. Eklund, Appl. Phys. Lett. (1991) 2678.

[7] M. S. Hybertsen and S. G. Louie, Phys. Rev. B **35** (1987) 5585.

[8] R. M. Pick *et al.*, Phys. Rev. B **1** (1970) 910.

[9] A. Baldereschi and E. Tosatti, Phys. Rev. B **17** (1978) 4710.

[10] J. L. Martins, N. Troullier, J. H. Weaver, Chem. Phys. Lett. **180** (1991) 457.

[11] M. Brack, Rev. Mod. Phys. **65** (1993) 677.

[12] F. Calogero, *Variable Phase approach to Potential Scattering*, AP, NY (1967); V. Babikov, *Method of the phase functions in quantum mechanics*, Nauka, Moscow (1971).

[13] S. Matt, B. Dunser, M. Lezius, H. Deutsch, A. K. Becker, B. A. Stamatovic, C. P. Scheier, T. D. Mark, J. Chem. Phys. **105**(1996) 1880.

[14] V. Foltin, M. Foltin, S. Matt, P. Scheier, K. Becker, H. Deutsch, T. D. Mark, Chem. Phys. Lett. **289** (1998) 181.

[15] S. Keller, E. Engel, Chem. Phys. Lett. **299** (1999) 165.

[16] S. Keller, Eur. Phys. J. D **13** (2001) 51.

[17] O. Kidun, J. Berakdar, Phys. Rev. Lett. **87** (2001) 263401.

[18] O. Kidun, J. Berakdar, Surf. Sci. **507-510** (2002) 662.

[19] O. Kidun, N. Fominykh, J. Berakdar, J. Phys. A, **35** (2002) 9413.